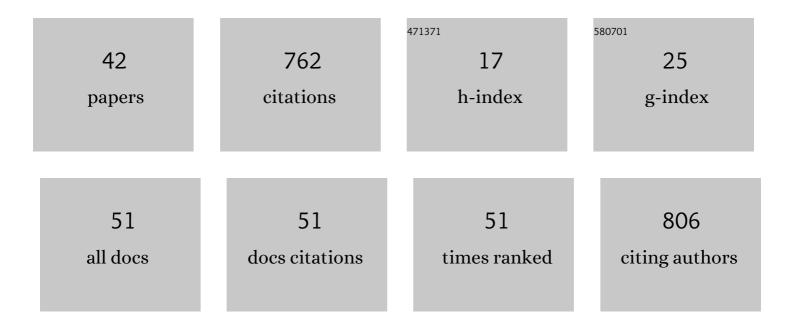
Laura Gomez

List of Publications by Year in descending order

Source: https://exaly.com/author-pdf/5580932/publications.pdf Version: 2024-02-01



LAURA COMEZ

#	Article	IF	CITATIONS
1	Radiation and Dust Sensor for Mars Environmental Dynamic Analyzer Onboard M2020 Rover. Sensors, 2022, 22, 2907.	2.1	18
2	New observations of NO ₂ in the upper troposphere from TROPOMI. Atmospheric Measurement Techniques, 2021, 14, 2389-2408.	1.2	18
3	Polar Stratospheric Clouds Detection at Belgrano II Antarctic Station with Visible Ground-Based Spectroscopic Measurements. Remote Sensing, 2021, 13, 1412.	1.8	6
4	Patterns and trends of ozone and carbon monoxide at Ushuaia (Argentina) observatory. Atmospheric Research, 2021, 255, 105551.	1.8	0
5	Intercomparison of MAX-DOAS vertical profile retrieval algorithms: studies on field data from the CINDI-2 campaign. Atmospheric Measurement Techniques, 2021, 14, 1-35.	1.2	32
6	Cirrus-induced shortwave radiative effects depending on their optical and physical properties: Case studies using simulations and measurements. Atmospheric Research, 2020, 246, 105095.	1.8	2
7	Intercomparison of NO ₂ , O ₄ , O ₃ and HCHO slant column measurements by MAX-DOAS and zenith-sky UV–visible spectrometers during CINDI-2. Atmospheric Measurement Techniques. 2020. 13. 2169-2208.	1.2	52
8	Inter-comparison of MAX-DOAS measurements of tropospheric HONO slant column densities and vertical profiles during the CINDI-2 campaign. Atmospheric Measurement Techniques, 2020, 13, 5087-5116.	1.2	18
9	Atmospheric formaldehyde at El Teide and Pic du Midi remote high-altitude sites. Atmospheric Environment, 2020, 234, 117618.	1.9	1
10	Is a scaling factor required to obtain closure between measured and modelled atmospheric O ₄ absorptions? An assessment of uncertainties of measurements and radiative transfer simulations for 2 selected days during the MAD-CAT campaign. Atmospheric Measurement Techniques, 2019, 12, 2745-2817.	1.2	22
11	Cirrus clouds properties derived from polarized micro pulse lidar (p-mpl) observations at the atmospheric observatory â€~el arenosillo' (sw iberian peninsula): a case study for radiative implications. EPJ Web of Conferences, 2018, 176, 05042.	0.1	0
12	Reactive bromine in the low troposphere of Antarctica: estimations at two research sites. Atmospheric Chemistry and Physics, 2018, 18, 8549-8570.	1.9	12
13	Measurement of dust optical depth using the solar irradiance sensor (SIS) onboard the ExoMars 2016 EDM. Planetary and Space Science, 2017, 138, 33-43.	0.9	15
14	DREAMS-SIS: The Solar Irradiance Sensor on-board the ExoMars 2016 lander. Advances in Space Research, 2017, 60, 103-120.	1.2	14
15	Investigating differences in DOAS retrieval codes using MAD-CAT campaign data. Atmospheric Measurement Techniques, 2017, 10, 955-978.	1.2	20
16	Vertical mass impact and features of Saharan dust intrusions derived from ground-based remote sensing in synergy with airborne in-situ measurements. Atmospheric Environment, 2016, 142, 420-429.	1.9	12
17	NO ₂ seasonal evolution in the north subtropical free troposphere. Atmospheric Chemistry and Physics, 2015, 15, 10567-10579.	1.9	9
18	Long-path averaged mixing ratios of O ₃ and NO ₂ in the free troposphere from mountain MAX-DOAS. Atmospheric Measurement Techniques, 2014, 7, 3373-3386.	1.2	17

LAURA GOMEZ

#	Article	IF	CITATIONS
19	Multi-platform in-situ and remote sensing techniques to derive Saharan dust properties during AMISOC-TNF 2013. , 2014, , .		0
20	Temperature dependences of air-broadening, air-narrowing and line-mixing coefficients of the methane ν23 R(6) manifold lines—Application to in-situ measurements of atmospheric methane. Journal of Quantitative Spectroscopy and Radiative Transfer, 2014, 133, 206-216.	1.1	21
21	lodine monoxide in the north subtropical free troposphere. Atmospheric Chemistry and Physics, 2012, 12, 4909-4921.	1.9	44
22	Comparison of quantum, semi-classical and classical methods in the calculation of nitrogen self-broadened linewidths. Journal of Quantitative Spectroscopy and Radiative Transfer, 2012, 113, 1887-1897.	1.1	27
23	Collisional line widths of autoperturbed N2: Measurements and quantum calculations. Journal of Quantitative Spectroscopy and Radiative Transfer, 2011, 112, 2542-2551.	1.1	21
24	Spectroscopy of CH4 with a difference-frequency generation laser at 3.3 micron for atmospheric applications. Applied Physics B: Lasers and Optics, 2011, 104, 989-1000.	1.1	19
25	Theoretical calculation of CH3Br/N2-broadening coefficients at various temperatures. Journal of Quantitative Spectroscopy and Radiative Transfer, 2011, 112, 769-778.	1.1	11
26	Comparison of classical, semiclassical and quantum methods in hydrogen broadening of acetylene lines. Journal of Quantitative Spectroscopy and Radiative Transfer, 2011, 112, 1429-1437.	1.1	17
27	Comparison of quantum, semiclassical and classical methods in hydrogen broadening of nitrogen lines. Journal of Quantitative Spectroscopy and Radiative Transfer, 2011, 112, 1942-1949.	1.1	17
28	Measurement of absolute line intensities in the ν5–ν4 band of 12C2H2 using SOLEIL synchrotron far infrared AILES beamline. Journal of Quantitative Spectroscopy and Radiative Transfer, 2010, 111, 1223-1233.	1.1	14
29	Theoretical calculations of self-broadening coefficients in the $\hat{1}$ /26 band of CH3Br. Journal of Quantitative Spectroscopy and Radiative Transfer, 2010, 111, 1252-1261.	1.1	19
30	New line intensity measurements for 12C2H2 around 7.7μm and HITRAN format line list for applications. Journal of Quantitative Spectroscopy and Radiative Transfer, 2010, 111, 2256-2264.	1.1	15
31	Line mixing calculation in the ν6 Q-branches of N2-broadened CH3Br at low temperatures. Journal of Molecular Spectroscopy, 2009, 256, 35-40.	0.4	15
32	New Analysis of the ν3 fundamental band of HDCO: Positions and intensities. Journal of Molecular Spectroscopy, 2009, 256, 28-34.	0.4	3
33	Some improvements of the HNO3 spectroscopic parameters in the spectral region from 600 to 950cmâ^'1. Journal of Quantitative Spectroscopy and Radiative Transfer, 2009, 110, 675-686.	1.1	17
34	Validation of HNO3 spectroscopic parameters using atmospheric absorption and emission measurements. Journal of Quantitative Spectroscopy and Radiative Transfer, 2009, 110, 109-117.	1.1	6
35	Theoretical calculations of N2-broadened half-widths of ν5 transitions of HNO3. Journal of Quantitative Spectroscopy and Radiative Transfer, 2009, 110, 687-699.	1.1	9
36	Line intensities of 12C2H2 in the 7.7μm spectral region. Journal of Quantitative Spectroscopy and Radiative Transfer, 2009, 110, 2102-2114.	1.1	17

LAURA GOMEZ

#	Article	IF	CITATIONS
37	N ₂ H ₂ isotropic Raman Qâ€branch linewidths: an Energyâ€Corrected Sudden scaling law. Journal of Raman Spectroscopy, 2008, 39, 707-710.	1.2	10
38	A bond–bond description of the intermolecular interaction energy: the case of weakly bound N2–H2 and N2–N2 complexes. Physical Chemistry Chemical Physics, 2008, 10, 4281.	1.3	78
39	Collisional line widths of autoperturbed N[sub 2]: measurements and quantum calculations. , 2008, , .		0
40	Q-branch linewidths of N2 perturbed by H2: Experiments and quantum calculations from an ab initio potential. Journal of Chemical Physics, 2007, 126, 204302.	1.2	27
41	Global fits of new intermolecular ground state potential energy surfaces for N2–H2 and N2–N2 van der Waals dimers. Chemical Physics Letters, 2007, 445, 99-107.	1.2	62
42	Theoretical and experimental analysis of N2–H2 stimulated Raman spectra. Molecular Physics, 2006, 104, 1869-1878.	0.8	8